

K63 ubiquitin chains target NLRP3 inflammasome for autophagic degradation in ox-LDL-stimulated THP-1 macrophages

Zhenfeng Zhou^{1,*}, Xiaoyan Zhu^{2,*}, Ruihua Yin¹, Tianwei Liu³, Shaonan Yang¹, Lingyan Zhou¹, Xudong Pan^{1,3}, Aijun Ma^{1,3}

¹Department of Neurology, the Affiliated Hospital of Qingdao University, Qingdao 266000, Shandong, China

²Department of Intensive Care Unit, the Affiliated Hospital of Qingdao University, Qingdao 266000, Shandong, China

³Institute of Cerebrovascular Diseases, the Affiliated Hospital of Qingdao University, Qingdao 266000, Shandong, China

*Equal contribution

Correspondence to: Aijun Ma, Xudong Pan; email: drmaj@126.com, drpan022@163.com

Keywords: atherosclerosis, NLRP3 inflammasome, autophagy, p62, K63 polyubiquitination

Received: August 23, 2019

Accepted: January 2, 2020

Published: January 29, 2020

Copyright: Zhou et al. This is an open-access article distributed under the terms of the Creative Commons Attribution License (CC BY 3.0), which permits unrestricted use, distribution, and reproduction in any medium, provided the original author and source are credited.

ABSTRACT

Inflammation, especially involving the NLRP3 inflammasome, is critical to atherosclerotic plaque formation. Enhanced autophagy can inhibit the development of atherosclerosis, and recent studies have revealed that NLRP3 inflammasome can be degraded by autophagy in atherosclerosis. In the present study, we established a foam-cell model to investigate the impact of oxidized low density lipoproteins (ox-LDLs) on autophagy and the inflammasome in atherosclerosis-related inflammation. We observed that ox-LDLs activated NLRP3 inflammasomes in macrophages and restricted autophagy in a time- and dose-dependent manner. We further observed through immunoprecipitation and siRNA knockdown that autophagic degradation of the NLRP3 inflammasome is dependent on K63 polyubiquitination of its NLRP3 subunit and subsequent binding by the adaptor protein p62. Our findings uncover a mechanism by which autophagy inhibits inflammation in atherosclerosis and the role of K63 in that process.

INTRODUCTION

Ischemic stroke is a debilitating and potentially lethal disease, and the leading cause of death in modern society. The main pathogenesis of ischemic stroke is considered to be atherosclerosis [1], a proven chronic inflammatory disease [2]. High levels of interleukin-1 β (IL-1 β), found in atherosclerotic artery specimens [3], accelerate the progression of atherosclerosis by activating endothelial cells and macrophages, which promote the generation of adhesion molecules that recruit leukocytes [4, 5] and stimulate smooth muscle cell proliferation [6]. Recent studies have demonstrated that increased IL-1 β in atherosclerotic plaque is primarily the result of activation of NLRP3 inflammasomes [7, 8]. Thus, exploring the

inflammatory mechanism of atherosclerosis and manipulating the function of NLRP3 inflammasomes have emerged as new approaches to understanding and treating the disease.

The NLRP3 inflammasome consists of three units: a sensor, nucleotide-binding domain and leucine-rich repeat protein-3 (NLRP3); an adaptor, apoptosis-associated speck-like protein containing a caspase recruitment domain (ASC); and an effector, protease caspase-1 [9]. When ligands bind to the leucine-rich repeat domain of NLRP3, NLRP3, ASC, and pro-caspase-1 oligomerize to form inflammasomes and convert dormant pro-caspase-1 into active caspase-1. This, in turn, processes pro-IL-1 β into mature IL-1 β [10, 11].

Autophagy is a highly conserved cellular process through which misfolded proteins and excessive signaling molecules are degraded by a structure known as the autophagosome, playing a crucial role in intracellular homeostasis and adaptation to environmental changes [12–14]. Autophagic adaptor protein p62 (SQSTM1) binds and targets the substrates of autophagosomes for degradation [15, 16]. However, autophagy itself is a non-specific system, and the recognition of its substrates by p62 requires the assistance of the ubiquitination system, which identifies and labels target proteins with specific ubiquitin chains, mainly lysine 63(K63) and lysine 48(K48) polyubiquitin chains [17, 18]. P62 discerns these polyubiquitin chains to identify its targets [19].

Recent studies have shown that autophagy can degrade inflammasomes to play an anti-inflammatory role, and the process involves ubiquitination of inflammasome constituent proteins. In a dsDNA-induced acute inflammatory cell model, autophagy identified K63 ubiquitinated ASC to degrade AIM2 inflammasomes (reactive inflammasomes of dsDNA) [20]. Dopamine promotes the autophagic degradation of NLRP3 inflammasomes by enhancing the K48-linked ubiquitination of NLRP3, thereby playing a protective role against Parkinson's disease, neuritis, and peritonitis [21]. NLRP3 inflammasomes are also autophagocytosed in atherosclerosis [22].

In the present study, a foam-cell model was established to investigate the impact of oxidized low density lipoproteins (ox-LDLs) on autophagy and inflammasomes, and the effect of autophagy on inflammation in atherosclerosis. Furthermore, we investigated the specific ubiquitin chain and molecular mechanism through which autophagy recognizes the NLRP3 inflammasome.

RESULTS

Ox-LDLs activate NLRP3 inflammasome in a time- and dose-dependent manner

In order to establish the foam-cell models, THP-1 derived macrophages (M ϕ) were stimulated with ox-LDLs for 24 hours, and stained with Oil Red O. As presented in Figure 1A and 1B, obvious lipid droplets were observed in ox-LDL-challenged M ϕ . In sharp contrast, no lipid droplet formation was observed in the control group.

In order to determine whether ox-LDLs activate NLRP3 inflammasomes, M ϕ were treated with ox-LDLs for a series of time intervals (0-48 hours) and concentrations (0-100 μ g/ml). Then, the expression of

NLRP3, ASC, pro-caspase-1, pro-IL-1 β , and activated caspase-1 (p20) in cell lysates was measured by western blot, while the expression of IL-1 β in the supernatants was determined by ELISA. We found that the expression of NLRP3 and pro-IL-1 β , and the production of activated caspase-1 (p20) (Figure 1C, 1D) and IL-1 β (Figure 1E) increased with the prolongation of stimulation time. Furthermore, the concentration gradient ox-LDL stimulation experiment revealed that the expression of NLRP3, pro-IL-1 β , and p20 (Figure 1F, 1G), and the level of supernatant IL-1 β (Figure 1H) were increased by ox-LDLs in a dose-dependent manner. Remarkably, the expression of ASC and pro-caspase-1 did not change in either experiment (Figure 1C and 1F).

These data indicate that ox-LDLs can activate NLRP3 inflammasomes, possibly by promoting the expression of NLRP3 and pro-IL-1 β . Consistent with the findings in LPS-induced inflammation models, the expression of ASC and pro-caspase-1 were not affected in the process [23]. Overall, these data suggest that ox-LDLs can activate the NLRP3 inflammasome in a time- and dose-dependent manner.

ox-LDLs restrict autophagy in a time- and dose-dependent manner

Next, the influence of ox-LDLs on autophagy was investigated. LC3II participates in the formation of autophagosomes, and increased LC3II/LCI ratio represents enhancement of autophagy. On the contrary, elevation of p62 indicates reduced autophagy [15]. The lysates from cells exposed to ox-LDLs in the previous experiment were subjected to western blot. As demonstrated in Figure 2A, the expression of p62 increased, and the LC3II/LCI ratio decreased with ox-LDL exposure in a time-dependent manner. Furthermore, the concentration gradient ox-LDL stimulation experiments revealed that the expression of p62 increased and the LC3II/LCI ratio decreased in a dose-dependent manner (Figure 2B). Overall, these results suggest that ox-LDLs suppress autophagy in a time- and dose-dependent manner.

Autophagy inhibits ox-LDL-induced NLRP3 inflammasome activation by degrading NLRP3 and ASC

Rapamycin, an autophagy enhancer, and 3-MA, an inhibitor, [24] were administered to M ϕ at one hour prior to ox-LDL stimulation. The western blot revealed that treatment with rapamycin decreased p62 in the cell lysates, but increased the LC3II/LCI ratio; conversely, treatment with 3-MA increased p62, but decreased the LC3II/LCI ratio (Figure 3A).

Next, we measured activated caspase-1 and mature IL-1 β in M ϕ , which had been treated with rapamycin or 3-MA and subsequently stimulated with ox-LDLs. Evidently, restricting autophagy with 3-MA resulted in

more inflammasome activity, as reflected by the increase in p20 and IL-1 β in cell lysates and the supernatant. Furthermore, the elevation of autophagy with rapamycin resulted in less inflammasome

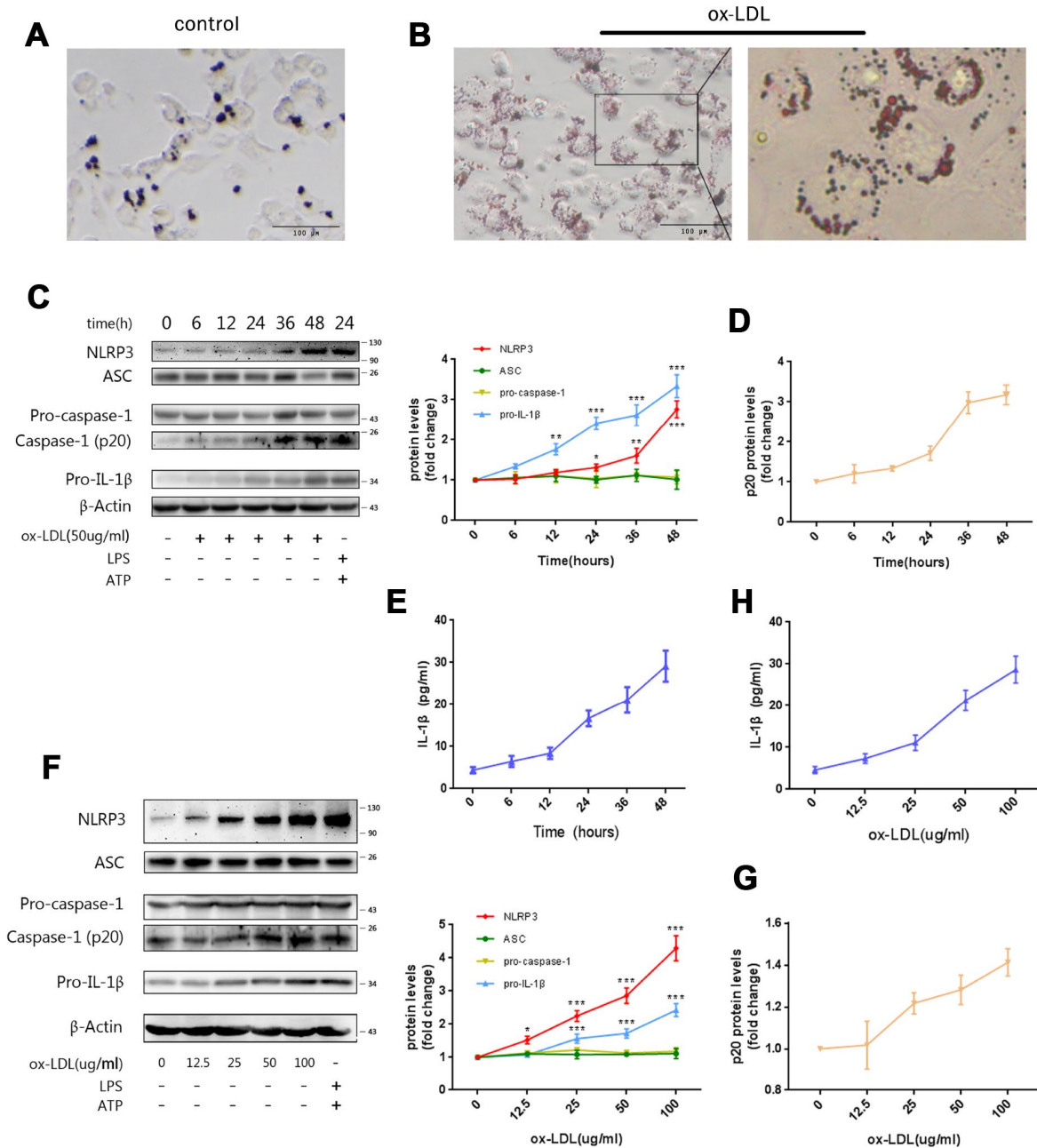


Figure 1. Ox-LDLs activate NLRP3 inflammasomes in a time- and dose-dependent manner. (A and B) Representative Oil Red O staining images of M ϕ treated with (B) or without (A) ox-LDLs. The right image in (B), 4 \times enlargement of the outlined area at the left. Scale bars, 100 μ m. (C) The immunoblot analysis of lysates of M ϕ treated with ox-LDLs (50 μ g/ml) for a series of time intervals. (C and D) The densitometric analysis of the NLRP3, ASC, pro-caspase-1, pro-IL-1 β (C) and p20 (D) signal vs. time, which was normalized to β -actin. (E) The ELISA of IL-1 β in supernatants obtained from (C). (F) The immunoblot analysis of lysates of M ϕ treated with various doses of ox-LDLs for 24 hours. (F and G) The densitometric analysis of the NLRP3, ASC, pro-caspase-1, pro-IL-1 β (F) and p20 (G) signal vs. ox-LDL concentrations, which were normalized to β -actin. (H) The ELISA of IL-1 β in supernatants obtained from (F). The data are presented as mean \pm SD ($n=3$); * denotes statistical significance by one-way analysis of variance (ANOVA) with *post hoc* Dunnett's multiple comparisons test when compared to 0 hour or 0 μ g/ml ox-LDLs. * $P<0.05$, ** $P<0.01$, *** $P<0.001$.

activity, as reflected by lesser p20 and IL-1 β (Figure 3B–3D). These data indicate that autophagy can regulate ox-LDL-induced NLRP3 inflammasome activation.

In order to further investigate the mechanism by which autophagy affects inflammasome activation, we measured the expression of NLRP3, ASC, pro-caspase-1 and pro-IL-1 β by western blot. As shown in Figure 3B, enhancing autophagy with rapamycin resulted in less NLRP3 and ASC, while blocking autophagy with 3-MA led to more NLRP3 and ASC in the cell lysates. However, the manipulation of autophagy did not cause significant changes in the expression of pro-caspase-1 and pro-IL-1 β . These data show that NLRP3 and ASC are regulated by autophagy. Next, bafilomycin A1, an autophagy inhibitor that blocks autophagosome-lysosome fusion, was administered to foam-cells to clarify whether NLRP3 and ASC were actually degraded by autophagy. As shown in Figure 3E, rapamycin dampened the expression of NLRP3 and ASC, while bafilomycin A1 elevated the expression of NLRP3 and ASC. This indicates that NLRP3 and ASC can be degraded *via* the autophagy process. In summary, these results suggest that autophagy may inhibit the activation of NLRP3 inflammasomes by degrading NLRP3 and ASC, but not pro-caspase-1 and pro-IL-1 β .

P62 is essential for autophagic degradation of NLRP3 inflammasomes

P62 is an important adaptor protein in autophagy, which identifies, binds, and targets substrates to the autophagosome for degradation [16]. In order to verify whether p62 mediates the recognition of NLRP3 inflammasomes by autophagy, p62-siRNA was transfected into M ϕ . Cell lysates from M ϕ transfected with p62-siRNA contained less p62 (Figure 4A) than controls. The ablation of p62 with siRNA in foam-cells led to more NLRP3, ASC (Figure 4B), and p20 (Figure 4B and 4C) in the cell lysates and IL-1 β (Figure 4D) in the supernatants, when compared to the control siRNA group; this was similar to the effects of 3-MA and bafilomycin A1.

In order to further evaluate the role of p62 in autophagy and inflammation, rapamycin was administered to M ϕ transfected with p62-siRNA at one hour prior to ox-LDL stimulation. As shown in Figure 4B–4D, the expression of NLRP3, ASC and p20 in the cell lysates, and the level of IL-1 β in the supernatants were not depressed by rapamycin, indicating that the effect of rapamycin in limiting inflammation by triggering autophagy was blocked. Overall, these data suggest that p62 plays an important role in the foam-cell model, and mediates the regulation of NLRP3 inflammasome by autophagy.

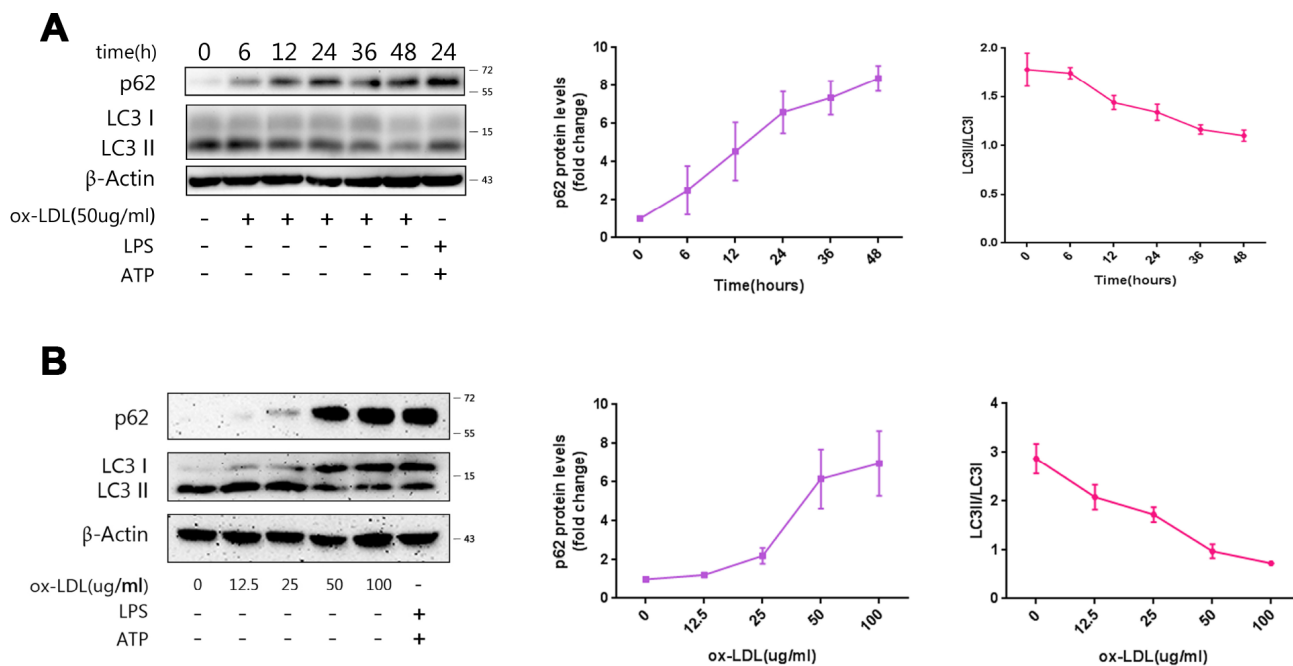


Figure 2. Ox-LDLs inhibit autophagy in a time- and dose-dependent manner. (A) The immunoblot analysis of lysates of M ϕ treated with ox-LDLs (50 ug/ml) for a series of time intervals. (B) The immunoblot analysis of lysates of M ϕ treated with various doses of ox-LDLs for 24 hours. (A and B) The densitometric analysis of the p62 signal and LC3II/LC3I ratio vs. time (A) and ox-LDL concentrations (B), which was normalized to β -actin. The data are presented as mean \pm SD ($n=3$).

NLRP3 is the main target of p62

According to the present results, the expression of NLRP3 and ASC, rather than pro-caspase-1 and pro-IL-1 β ,

significantly vary with the manipulation of autophagy, which implies that NLRP3 and ASC are targets of autophagy. Previous studies have shown that both NLRP3 and ASC can interact and co-localize with

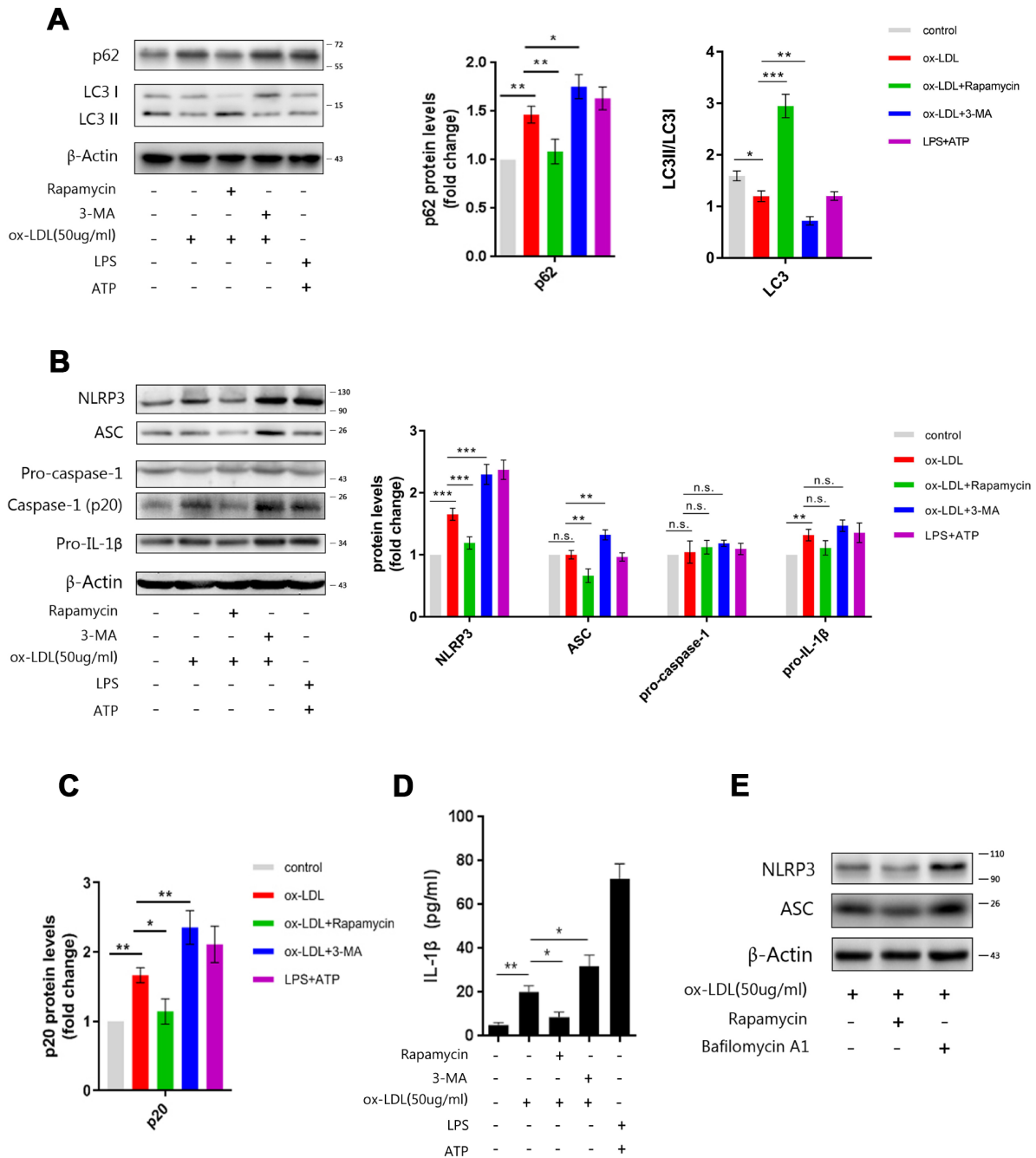


Figure 3. Manipulating the autophagy affects NLRP3 inflammasomes. (A) The immunoblot analysis of lysates of M ϕ , which were left untreated or treated with rapamycin or 3-MA, and subsequently stimulated with ox-LDLs (50 ug/ml), or LPS and ATP for 24 hours. (B) The immunoblot analysis of lysates of M ϕ , which were left untreated or treated with rapamycin or 3-MA, and subsequently stimulated with ox-LDLs (50 ug/ml), or LPS and ATP for 24 hours. (A–C) The densitometric analysis of the p62 signal and LC3II/LC3I ratio (A), the NLRP3, ASC, pro-caspase-1 and pro-IL-1 β signal (B), which were normalized to β -actin. (D) The ELISA of IL-1 β in the supernatants obtained from (B). (E) The immunoblot analysis of lysates of M ϕ , which were left untreated or treated with rapamycin or bafilomycin A1, and subsequently stimulated with ox-LDLs (50 ug/ml) for 24 hours. The data are presented as mean \pm SD ($n=3$); * denotes the statistical significance by one-way ANOVA with *post hoc* Dunnett's multiple comparisons test. * $P<0.05$, ** $P<0.01$, *** $P<0.001$.

p62 alone [20, 25]. So, immunoprecipitation was performed to clarify whether NLRP3 or ASC is the major target of autophagy, or whether they play equal roles in mediating the autophagic degradation of NLRP3 inflammasomes. As shown in Figure 5, both NLRP3 and ASC were immunoprecipitated from cell lysates with the p62 antibody (Figure 5A). When the cell lysates were immunoprecipitated with NLRP3 or ASC antibodies, the ratios of NLRP3 to ASC obtained from the NLRP3 and the ASC immunoprecipitates were the same (Figure 5A and 5B). These results indicate that there is a stable combination between NLRP3 and ASC and rules out the influence of the disassembly of NLRP3 and ASC on p62. However, more p62 was detected in the NLRP3 immunoprecipitates than in the ASC immunoprecipitates (Figure 5A). This trend was more significant when the signals of p62 obtained from the NLRP3 immunoprecipitates or the ASC immunoprecipitates were normalized to NLRP3 or ASC, respectively (Figure 5C). These results indicate that more p62 detached from the NLRP3 and ASC complex

during ASC immunoprecipitation and the combination of p62 to the NLRP3 and ASC complex is preserved better when immunoprecipitated with NLRP3 antibodies. These results suggest that NLRP3 may be the major or direct target of p62.

P62 binds to NLRP3 *via* the K63 polyubiquitin chains

We next sought to determine how p62 recognizes NLRP3 inflammasomes. P62 contains an ubiquitin binding domain (UBA). Hence, immunoprecipitation was performed to determine whether NLRP3 or ASC was ubiquitinated in ox-LDL-stimulated Mφ. As shown in Figure 6A, both lysine 48 (K48)- and lysine 63 (K63)-linked polyubiquitin chains were detected in the NLRP3 and ASC immunoprecipitates obtained from foam-cell lysates. Ablating p62 with p62-siRNA increased the NLRP3 and ASC expression (Figure 6B). Further investigation revealed that the K63, rather than the K48, polyubiquitin chains dramatically accumulated

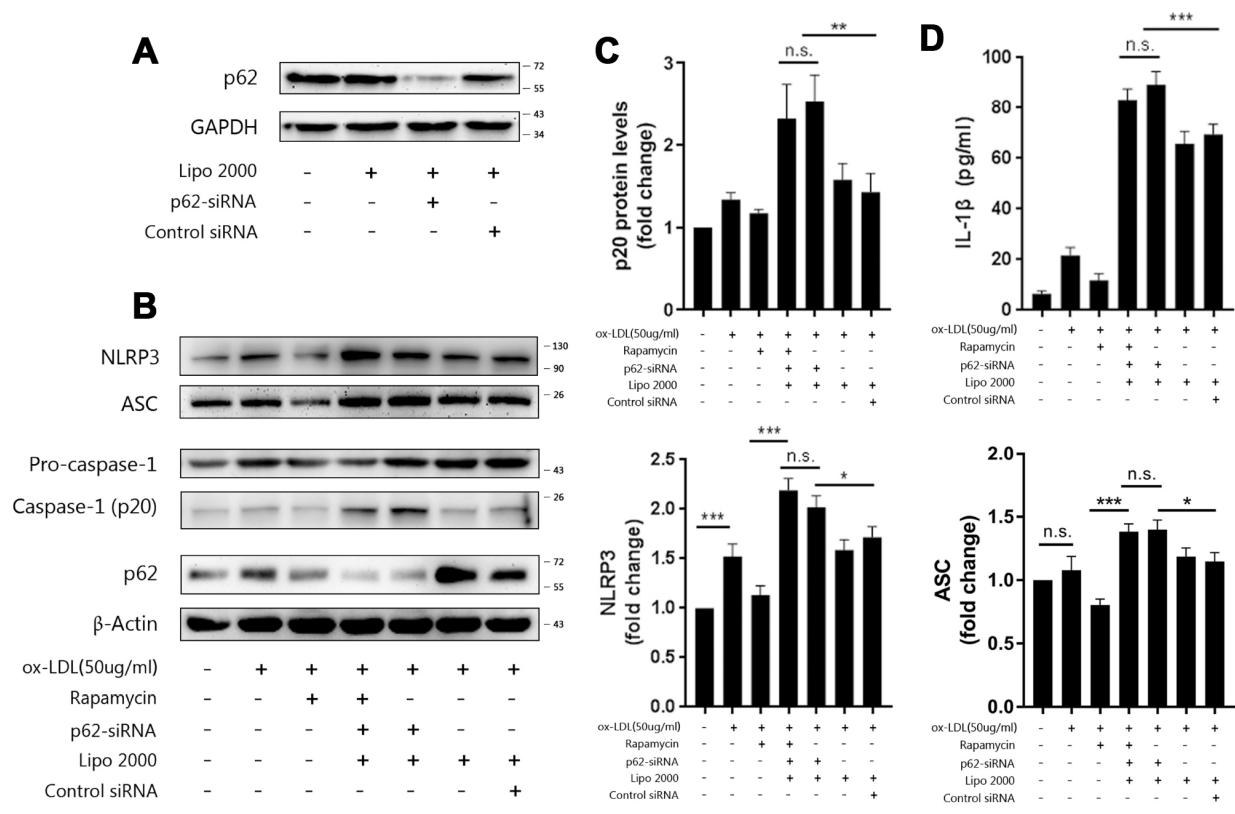


Figure 4. P62 mediates the autophagic regulation of NLRP3 inflammasomes. (A) The expression of p62 in the lysates of Mφ, which were left untransfected or transfected with vehicle, p62-siRNA, or control siRNA for 48 hours. (B) The immunoblot analysis of the lysates of Mφ, which were left untransfected or transfected with vehicle, p62-siRNA, or control siRNA for 24 hours, and subsequently treated with or without rapamycin, and stimulated with ox-LDLs (50 ug/ml) for another 24 hours. Rapamycin was administered to cells for one hour prior to ox-LDL stimulation. (B and C) The densitometric analysis of the NLRP3, ASC, (B) and p20 (C) signal, which were normalized to β-actin. (D) The ELISA of IL-1β in the supernatants obtained from (B). The data are presented as mean ± SD (n=3); * denotes the statistical significance by one-way ANOVA with *post hoc* Dunnett's multiple comparisons test. *P<0.05, **P<0.01, ***P<0.001.

on NLRP3 when p62-siRNA was transfected into M ϕ . Furthermore, the K48 and K63 polyubiquitin chains that attached to ASC did not significantly change, when compared with the control siRNA groups (Figure 6C). Interestingly, it was found that ox-LDL stimulation slightly reduced the K48 and K63 ubiquitin chains attached to NLRP3 (Figure 6D). This is consistent with the discovery that NLRP3 undergoes de-ubiquitination during NLRP3 inflammasome activation [26]. These data suggest that the accumulation of K63 polyubiquitin chains on NLRP3 is a specific result of the p62 ablation. These results indicate that K63 polyubiquitin chains play an important role in the binding of p62 to NLRP3, and further confirm that NLRP3 is the main target of p62 in the autophagic regulation process of inflammation.

In order to further certify these findings, AMSH (an associated molecule with an Src homology 3 domain of the signal transducing adaptor molecule), which is a K63-linked polyubiquitin chain-specific deubiquitinating enzyme [27], was used to trim the K63 polyubiquitin chains on NLRP3. First, immunoblotting

was performed, and it was found that AMSH hydrolyzed the K63 polyubiquitin chains without affecting the K48 polyubiquitin chains (Figure 6E) or NLRP3 (Figure 6F). Next, the NLRP3 immunoprecipitates were treated with AMSH. Consistent with the previous results, AMSH ablated the K63 polyubiquitin chains in the precipitates, while the K48 polyubiquitin chains were exempted (Figure 6G). Finally, the p62 immunoprecipitates were pretreated with AMSH, and less NLRP3 was detected by western blot than in the control group (Figure 6H). Overall, these results indicate that p62 mediates the regulation of NLRP3 inflammasomes through autophagy by recognizing the K63 polyubiquitin chains on NLRP3.

DISCUSSION

The present study uncovered the molecular mechanism and role of ubiquitination in mediating the identification of NLRP3 inflammasomes by autophagy. In the foam-cell models, ox-LDLs on their own activated NLRP3 inflammasomes and restricted autophagy. Meanwhile,

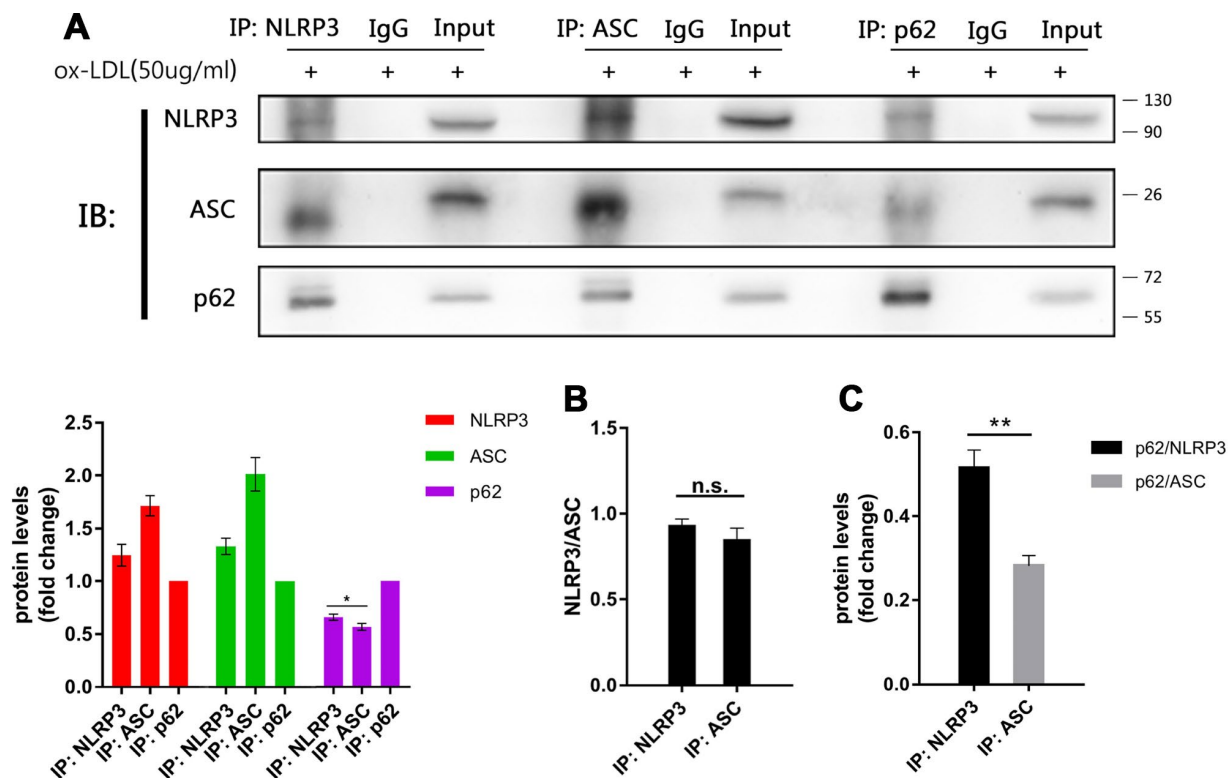


Figure 5. The main target of p62 is more likely to be NLRP3. (A above) The immunoblot analysis of the NLRP3, ASC and p62 immunoprecipitates of cell lysates obtained from M ϕ , which had been stimulated with ox-LDLs (50 ug/ml) for 24 hours. (A below) The densitometric analysis of the NLRP3, ASC and p62 signal, which were normalized to the corresponding signals in the p62 immunoprecipitates. (B) The densitometric analysis of the ratios of NLRP3/ASC obtained from the NLRP3 immunoprecipitates and the ASC immunoprecipitates. (C) The densitometric analysis of p62 signal detected in the NLRP3 immunoprecipitates and the ASC immunoprecipitates, and normalized to the corresponding NLRP3 and ASC signal respectively. The data are presented as mean \pm SD ($n=3$); * denotes the statistical significance by one-way ANOVA with *post hoc* Dunnett's multiple comparisons test (A) or by t-test (B and C). * $P<0.05$, ** $P<0.01$, *** $P<0.001$.

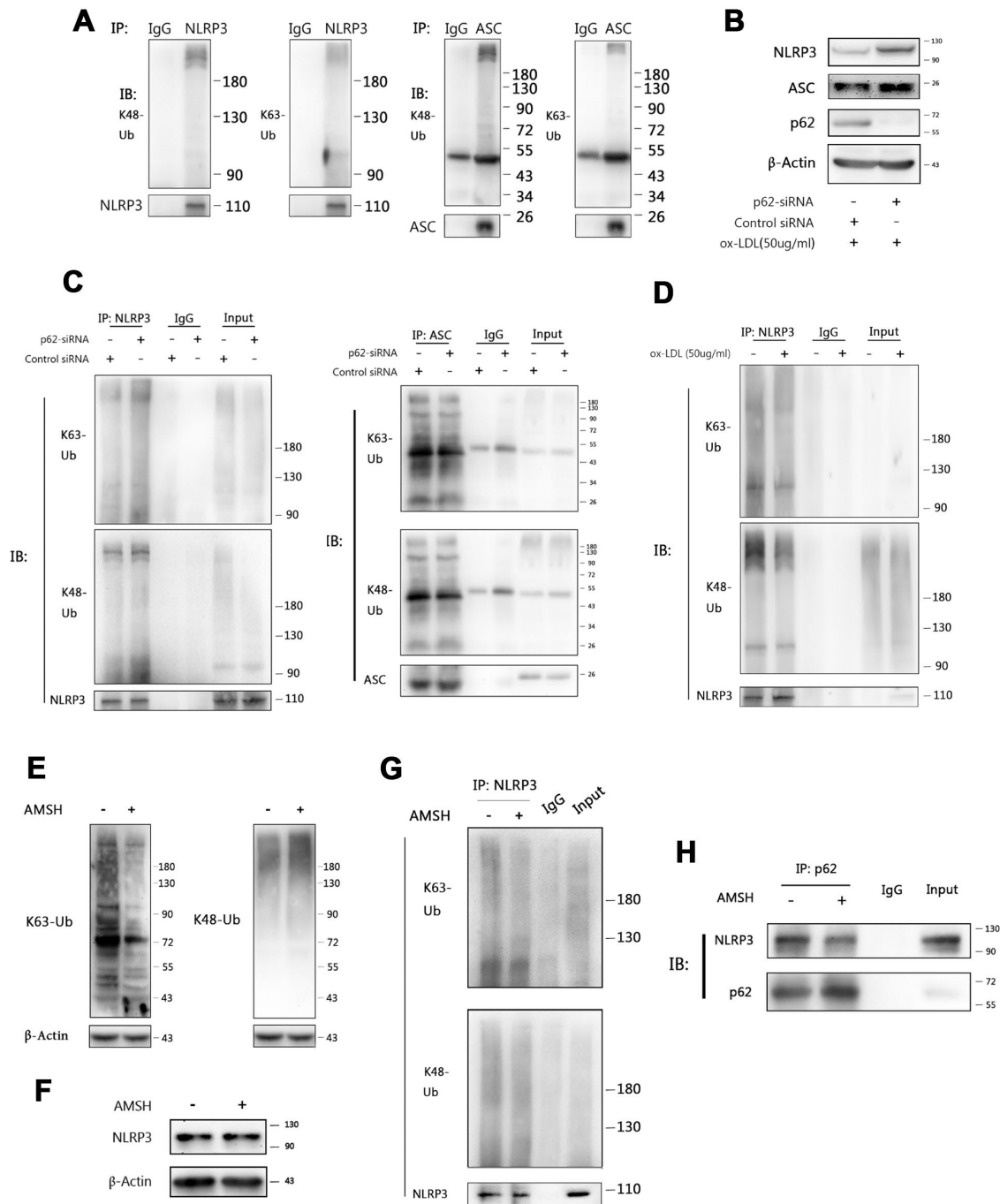


Figure 6. P62 binds to NLRP3 via the K63 polyubiquitin chains. (A) The immunoblot analysis of NLRP3 and ASC immunoprecipitates of M ϕ stimulated with ox-LDLs (50 ug/ml) for 24 hours. (B) The immunoblot analysis of the total lysates of M ϕ transfected with control siRNA or p62-siRNA for 24 hours, and subsequently stimulated with ox-LDLs (50 ug/ml) for another 24 hours. (C) The immunoblot analysis of NLRP3 (left) and ASC (right) immunoprecipitates of M ϕ treated as described in (B). (D) The immunoblot analysis of NLRP3 immunoprecipitates of M ϕ treated with or without ox-LDL (50 ug/ml) for 24 hours. (E) The detection for K63 (left) and K48 (right) polyubiquitin chains in the total foam-cell lysates pretreated with or without AMSH by immunoblotting. Prior to immunoblotting, 50 μ l of ox-LDL stimulated M ϕ lysates were administered with or without 1 μ l of AMSH (AMSH concentration: 500 nM), and incubated at 37°C for 30 minutes. (F) The immunoblot analysis of NLRP3 and β -Actin in the total foam-cell lysates pretreated with or without AMSH (500 nM), as described in (E). (G) The NLRP3 immunoprecipitates obtained from ox-LDL stimulated M ϕ lysates were treated with or without AMSH (500 nM), as described in (E), and subsequently subjected to immunoblotting. (H) The p62 immunoprecipitates obtained from foam-cell lysates were treated with or without AMSH (500 nM), as described in (E), and subsequently subjected to immunoblotting. All experiments were independently repeated for at least three times.

regulation of NLRP3 inflammasomes is mediated by the autophagy adaptor protein p62 and that this process was achieved through the recognition of p62 to the K63 ubiquitin chains on the NLRP3 protein.

The effect of ox-LDLs on NLRP3 inflammasomes has long been under discussion. One possible mechanism by which ox-LDLs activate NLRP3 inflammasomes is that ox-LDLs promote the production of cholesterol crystals, which in turn induce the expression and activation of NLRP3 inflammasomes [7]. However, ox-LDLs also inhibit LPS-induced inflammation by blocking the binding of NF- κ B to the DNA in a dose-dependent manner [28]. Yury I. Miller hypothesized that low level and transient ox-LDL stimulation dampens the inflammatory response. However, under conditions of hyperlipidemia, the increased and prolonged production of ox-CE and ox-PE (oxidized cholesteryl esters and oxidized phosphatidylethanolamine, the components of ox-LDLs) may result in chronic inflammation [29]. It was demonstrated in the present study that ox-LDLs activate NLRP3 inflammasomes in a time- and dose-dependent manner, and long-term ox-LDL stimulation activates NLRP3 inflammasomes, even when the stimulating concentration is lower than 10 μ g/ml.

The finding that inflammasome itself can be regulated by autophagy is a new discovery in recent years [14]. In dsDNA stimulated macrophages, autophagy has been reported to be able to degrade ASC to block the assembly of AIM2 inflammasomes [20]. Autophagy has also been proven to engulf NLRP3 to play an anti-inflammatory role in Parkinson's disease [21]. Furthermore, we found in ox-LDL-induced foam-cells that autophagy regulates inflammation by degrading the NLRP3 inflammasome subunit--NLRP3 and ASC. Further investigation revealed that the main target of autophagy is more likely to be NLRP3, because the combination of p62 to the NLRP3 and ASC complex is preserved better when immunoprecipitated with NLRP3 antibodies and that the ubiquitination modification on ASC remains unchanged after knocking down the expression of p62.

The role of p62 is crucial for autophagy to identify substrates. Mutations in the ubiquitin associated domain (UBA) deprive p62 of the ability to recognize K48 polyubiquitin chains, resulting in Paget's disease [30]. Autophagy moderates atherosclerosis by engulfing misfolded proteins bounded by p62 [31]. Recent studies have revealed that p62 efficiently targets proteins labeled by two or more ubiquitin chains composed of at least three ubiquitin moieties, and crosses link with each other to cluster substrates [32]. This is the result of the viscous liquid-like properties of p62, which promote a phase separation after p62 covalently combines with the

ubiquitin chains attached on the substrates. These cargos further recruit LC3 and drive the assembly of autophagosome around themselves [33]. In agreement with these findings, we found that autophagy regulates NLRP3 inflammasomes in atherosclerosis through the binding of p62 to NLRP3, since depleting p62 blocks the NLRP3 inflammasome regulating effect of autophagy, and reversing the anti-inflammatory role of rapamycin.

Ubiquitination has been proven to participate in the activation and degradation of inflammasomes. G5, which is a small molecule inhibitor of deubiquitination, critically regulates inflammasome activity by dampening the deubiquitination of NLRP3 [26]. The K63 polyubiquitin modification of pro-IL-1 β has been considered as a prerequisite for the binding of activated caspase-1 to pro-IL-1 β [27]. Furthermore, the K48 ubiquitination of NLRP3 promotes its proteasomal degradation [34]. It appears that the function of ubiquitination varies with the ubiquitin chain types and the proteins targeted. In the present study, it was revealed that ablating p62 results in increase in K63 polyubiquitin chains attached to NLRP3, and the disassembly of K63 polyubiquitin chains on NLRP3 with AMSH, leading to decreased NLRP3 binding with p62. These results suggest that the autophagic adaptor protein p62 detects NLRP3 by identifying the accumulated K63 polyubiquitin chains on it. The slightly longer K48 polyubiquitin chains on NLRP3, when ablating p62 with p62-siRNA, may be the result of the compensatory increase of proteasome degradation.

In summary, we demonstrated that in ox-LDL-stimulated foam-cells, ox-LDLs activate NLRP3 inflammasomes while inhibiting autophagy, which exacerbates the inflammatory response in foam-cells. Manipulating autophagy could be an effective approach to regulate the function of NLRP3 inflammasomes. It is noteworthy that the possible mechanism is that the autophagy engulfs NLRP3 *via* the recognition by p62 of the K63 ubiquitin chains on NLRP3. This NLRP3 inflammasome-regulating mechanism may help lead to development of specific activators or inhibitors, and fruitful atheroprotective measures in the future.

MATERIALS AND METHODS

Reagents and antibodies

ox-LDLs were purchased from Yiyuanbiotech (Guangzhou, China). Phorbol-12-myristate-13-acetate (PMA), rapamycin, 3-methyladenine (3-MA), bafilomycin A1 and protease inhibitor cocktails were purchased from MCE (Monmouth Junction, USA). LPS and ATP were purchased from Sigma (St Louis, MO),

USA). Lipofectamine™ 2000 was purchased from Invitrogen (Carlsbad, USA). Antibody to GAPDH, antibody to β -actin and HRP-conjugated secondary polyclonal antibodies to mouse and rabbit IgGs were purchased from Elabscience (Wuhan, China). Rabbit monoclonal anti-NLRP3, anti-ASC, anti-SQSTM1/p62, anti-LC3B, antibody to K63-linked polyubiquitin chains, antibody to K48-linked polyubiquitin chains and p62-siRNA, and control siRNA were purchased from Cell Signaling Technology (Boston, USA). Rabbit monoclonal anti-IL-1 β , anti-caspase-1 were purchased from Abcam (Cambridge, MA, USA). For the immunoprecipitation, polyclonal rabbit anti-SQSTM1/p62 was purchased from Abcam (Cambridge, MA, USA). Monoclonal mouse anti-SQSTM1/p62, anti-NLRP3, anti-ASC and protein A/G Plus-agarose were purchased from Santa Cruz Biotechnology (Santa Cruz, CA, USA). AMSH (the JAMM/MPN+ family of K63-specific DUB) was purchased from Boston Biochem (Cambridge, MA, USA).

Cell culture

Human THP-1 monocytes purchased from Shanghai Institutes for Biological Sciences (SIBS, Shanghai, China) were routinely cultured in 1640 medium supplemented with 10% fetal bovine serum (FBS; Biological Industries, Israel) and 1% penicillin-streptomycin (HyClone, USA) at 37°C with 5% CO₂. Prior to the experiments, THP-1 cells (4×10^5 cells/ml) were differentiated into macrophages with 25 ng/ml of PMA for 24 hours, and incubated in fresh culture medium for another 24 hours. These cells were referred to as THP-1 M ϕ . M ϕ were treated with 50 μ g/ml of ox-LDLs for 24 hours, or according to the concentration and time indicated in the specific experiment to establish the foam-cells model. In autophagy modulation experiments, 25 nM of rapamycin, 5 mM of 3-MA or 15 nM bafilomycin A1 were administered to the M ϕ at one hour prior to ox-LDLs and incubated for 24 hours. LPS and ATP were used at concentration of 100 ng/ml and 5 mM, respectively.

Oil red O staining

Next, 2×10^5 cells/ml of THP-1 monocytes were seeded into 6-well plates and sequentially treated with PMA and ox-LDLs, as described. After 72 hours, these cells were rinsed with PBS twice, and fixed with 4% paraformaldehyde for 25 minutes. Then, these cells were rinsed with 60% isopropanol for 15 seconds, stained with Oil Red O working solution for 30 minutes at 37°C, and rinsed with PBS twice and 60% isopropanol for 10 seconds, successively. Afterwards, these cells were immediately rinsed with PBS again, and photographed under a microscope.

Transfection with siRNA

THP-1 cells were seeded at a density of 5×10^5 cells/ml, differentiated with PMA, as described, and incubated in antibiotic-free medium for 24 hours. Lipofectamine™ 2000 was used according to manufacturer's instructions to transfect the siRNA for six hours. Then, these cells were cultured in antibiotic-free medium for 18 hours prior to subsequent experiments.

Enzyme-linked immunosorbent assay (ELISA)

The IL-1 β level in the cell culture supernatant was determined using IL-1 β ELISA Kits (Elabscience, Wuhan, China), and performed according to manufacturer's instructions.

Western blot

Cells were lysed on ice with standard RIPA buffer containing PMSF and a protease inhibitor cocktail for 30 minutes. After centrifugation for 10 minutes at 4°C, the supernatants were collected and subjected to 6-12% SDS-polyacrylamide gel electrophoresis. Then, the protein samples on the gel were transferred onto polyvinylidene difluoride membranes (Millipore Co, NJ, USA). After blocking in 5% skim milk at room temperature for 1.5 hours, these membranes were incubated with the appropriate primary antibody overnight at 4°C. The next day, the membranes were washed with TBST thrice, and incubated with HRP-conjugated anti-rabbit or mouse IgG antibodies for 1.5 hours at room temperature. Then, the bands were developed using Pierce ECL (Millipore Co, NJ, USA), and the images were gathered and analyzed using the NIH Image J software.

Immunoprecipitation

4×10^6 cells in 10-cm dishes were lysed on ice in lysis buffer (20 mM of Tris [pH 7.5], 150 mM of NaCl, and 1% Triton X-100) with PMSF and the protease inhibitor cocktail, and sonicated. Then, the lysates were incubated with the appropriate antibodies for 2-10 hours at 4°C prior to the addition of protein A/G Plus-agarose. Afterwards, the immunoprecipitates were collected and washed four times with the lysis buffer, and subjected to immunoblotting.

DUB assays

Cells in a 10-cm dish were lysed and immunoprecipitated with anti-p62, as previously described. The precipitates were washed three times with lysis buffer, and an additional two times with a reaction buffer (50 mM of Tris, pH 7.5, 150 mM of sodium chloride, 25

mM of potassium chloride, 5 mM of magnesium chloride and 1 mM of DTT). Then, the precipitates were collected and resuspended in 50 ul of reaction buffer, containing 1 ul of AMSH. After incubation at 37°C for 30 minutes, the precipitates were subjected to two washes, and heated in 2× loadingbuffer.

Statistical analysis

Data are presented as mean ± standard deviation (SD). All cell experiments were independently performed at least three times. All statistical analyses were performed using Graph Pad Prism 7 software (GraphPad Software, San Diego, CA, USA). $P < 0.05$ were considered statistically significant.

Abbreviations

THP-1 cells: human myeloid leukemia mononuclear cells; Ox-LDLs: oxidized low density lipoproteins; NLRP3: nucleotide-binding domain and leucine-rich repeats containing pyrin domain 3; ASC: the apoptosis-associated speck-like protein containing caspase recruitment domain; AMSH: associated molecule with a Src homology 3 domain of signal transducing adaptor molecule; siRNA: small interfering RNA.

ACKNOWLEDGMENTS

We thank Zhiyuan Li and Dr. Jisheng Zhang (Department of Otolaryngology-Head and Neck Surgery, Key Laboratory, The Affiliated Hospital of Qingdao University) for their help during the experiments.

CONFLICTS OF INTEREST

All authors report no financial or other conflicts of interest in relationship to the contents of this article.

FUNDING

This work was supported by the National Key R&D Program of China (No. 2017YFC1310903); and the National Natural Science Foundation of China (No. 81771259 and no. 81571112).

REFERENCES

1. Braunwald E. Shattuck lecture—cardiovascular medicine at the turn of the millennium: triumphs, concerns, and opportunities. *N Engl J Med.* 1997; 337:1360–69. <https://doi.org/10.1056/NEJM199711063371906> PMID:9358131
2. Libby P. Inflammation in atherosclerosis. *Arterioscler*

3. Thromb Vasc Biol. 2012; 32:2045–51. <https://doi.org/10.1161/ATVBAHA.108.179705> PMID:22895665
4. Galea J, Armstrong J, Gadsdon P, Holden H, Francis SE, Holt CM. Interleukin-1 beta in coronary arteries of patients with ischemic heart disease. *Arterioscler Thromb Vasc Biol.* 1996; 16:1000–06. <https://doi.org/10.1161/01.ATV.16.8.1000> PMID:8696938
5. Fearon WF, Fearon DT. Inflammation and cardiovascular disease: role of the interleukin-1 receptor antagonist. *Circulation.* 2008; 117:2577–79. <https://doi.org/10.1161/CIRCULATIONAHA.108.772491> PMID:18490534
6. Abbate A, Van Tassell BW, Biondi-Zoccai GG. Blocking interleukin-1 as a novel therapeutic strategy for secondary prevention of cardiovascular events. *BioDrugs.* 2012; 26:217–33. <https://doi.org/10.1007/BF03261881> PMID:22571369
7. Libby P, Warner SJ, Friedman GB. Interleukin 1: a mitogen for human vascular smooth muscle cells that induces the release of growth-inhibitory prostanoids. *J Clin Invest.* 1988; 81:487–98. <https://doi.org/10.1172/JCI113346> PMID:3276731
8. Duewell P, Kono H, Rayner KJ, Sirois CM, Vladimer G, Bauernfeind FG, Abela GS, Franchi L, Nuñez G, Schnurr M, Espevik T, Lien E, Fitzgerald KA, et al. NLRP3 inflammasomes are required for atherogenesis and activated by cholesterol crystals. *Nature.* 2010; 464:1357–61. <https://doi.org/10.1038/nature08938> PMID:20428172
9. Zhuang T, Liu J, Chen X, Zhang L, Pi J, Sun H, Li L, Bauer R, Wang H, Yu Z, Zhang Q, Tomlinson B, Chan P, et al. Endothelial Foxp1 Suppresses Atherosclerosis via Modulation of Nlrp3 Inflammasome Activation. *Circ Res.* 2019; 125:590–605. <https://doi.org/10.1161/CIRCRESAHA.118.314402> PMID:31318658
10. Schroder K, Tschopp J. The inflammasomes. *Cell.* 2010; 140:821–32. <https://doi.org/10.1016/j.cell.2010.01.040> PMID:20303873
11. Martinon F, Burns K, Tschopp J. The inflammasome: a molecular platform triggering activation of inflammatory caspases and processing of proIL-beta. *Mol Cell.* 2002; 10:417–26. [https://doi.org/10.1016/S1097-2765\(02\)00599-3](https://doi.org/10.1016/S1097-2765(02)00599-3) PMID:12191486
12. Wang L, Manji GA, Grenier JM, Al-Garawi A, Merriam S, Lora JM, Geddes BJ, Briskin M, DiStefano PS, Bertin J. PYPAF7, a novel PYRIN-containing Apaf1-like protein that regulates activation of NF-kappa B and caspase-1-

- dependent cytokine processing. *J Biol Chem.* 2002; 277:29874–80.
<https://doi.org/10.1074/jbc.M203915200>
PMID:12019269
12. Deretic V, Saitoh T, Akira S. Autophagy in infection, inflammation and immunity. *Nat Rev Immunol.* 2013; 13:722–37.
<https://doi.org/10.1038/nri3532> PMID:24064518
13. Kim KH, Lee MS. Autophagy—a key player in cellular and body metabolism. *Nat Rev Endocrinol.* 2014; 10:322–37.
<https://doi.org/10.1038/nrendo.2014.35>
PMID:24663220
14. Cadwell K. Crosstalk between autophagy and inflammatory signalling pathways: balancing defence and homeostasis. *Nat Rev Immunol.* 2016; 16:661–75.
<https://doi.org/10.1038/nri.2016.100> PMID:27694913
15. Pankiv S, Clausen TH, Lamark T, Brech A, Bruun JA, Outzen H, Øvervatn A, Bjørkøy G, Johansen T. p62/SQSTM1 binds directly to Atg8/LC3 to facilitate degradation of ubiquitinated protein aggregates by autophagy. *J Biol Chem.* 2007; 282:24131–45.
<https://doi.org/10.1074/jbc.M702824200>
PMID:17580304
16. Ponpuak M, Davis AS, Roberts EA, Delgado MA, Dinkins C, Zhao Z, Virgin HW 4th, Kyei GB, Johansen T, Vergne I, Deretic V. Delivery of cytosolic components by autophagic adaptor protein p62 endows autophagosomes with unique antimicrobial properties. *Immunity.* 2010; 32:329–41.
<https://doi.org/10.1016/j.immuni.2010.02.009>
PMID:20206555
17. Chau V, Tobias JW, Bachmair A, Marriott D, Ecker DJ, Gonda DK, Varshavsky A. A multiubiquitin chain is confined to specific lysine in a targeted short-lived protein. *Science.* 1989; 243:1576–83.
<https://doi.org/10.1126/science.2538923>
PMID:2538923
18. Jin L, Williamson A, Banerjee S, Philipp I, Rape M. Mechanism of ubiquitin-chain formation by the human anaphase-promoting complex. *Cell.* 2008; 133:653–65.
<https://doi.org/10.1016/j.cell.2008.04.012>
PMID:18485873
19. Khaminets A, Behl C, Dikic I. Ubiquitin-Dependent and Independent Signals In Selective Autophagy. *Trends Cell Biol.* 2016; 26:6–16.
<https://doi.org/10.1016/j.tcb.2015.08.010>
PMID:26437584
20. Shi CS, Shenderov K, Huang NN, Kabat J, Abu-Asab M, Fitzgerald KA, Sher A, Kehrl JH. Activation of autophagy by inflammatory signals limits IL-1 β production by targeting ubiquitinated inflammasomes for destruction. *Nat Immunol.* 2012; 13:255–63.
<https://doi.org/10.1038/ni.2215> PMID:22286270
21. Yan Y, Jiang W, Liu L, Wang X, Ding C, Tian Z, Zhou R. Dopamine controls systemic inflammation through inhibition of NLRP3 inflammasome. *Cell.* 2015; 160:62–73.
<https://doi.org/10.1016/j.cell.2014.11.047>
PMID:25594175
22. Peng S, Xu LW, Che XY, Xiao QQ, Pu J, Shao Q, He B. Atorvastatin Inhibits Inflammatory Response, Attenuates Lipid Deposition, and Improves the Stability of Vulnerable Atherosclerotic Plaques by Modulating Autophagy. *Front Pharmacol.* 2018; 9:438.
<https://doi.org/10.3389/fphar.2018.00438>
PMID:29773990
23. He Y, Hara H, Núñez G. Mechanism and Regulation of NLRP3 Inflammasome Activation. *Trends Biochem Sci.* 2016; 41:1012–21.
<https://doi.org/10.1016/j.tibs.2016.09.002>
PMID:27669650
24. Yang Z, Klionsky DJ. Mammalian autophagy: core molecular machinery and signaling regulation. *Curr Opin Cell Biol.* 2010; 22:124–31.
<https://doi.org/10.1016/j.ceb.2009.11.014>
PMID:20034776
25. Mehto S, Jena KK, Nath P, Chauhan S, Kolapalli SP, Das SK, Sahoo PK, Jain A, Taylor GA, Chauhan S. The Crohn's Disease Risk Factor IRGM Limits NLRP3 Inflammasome Activation by Impeding Its Assembly and by Mediating Its Selective Autophagy. *Mol Cell.* 2019; 73:429–445.e7.
<https://doi.org/10.1016/j.molcel.2018.11.018>
PMID:30612879
26. Py BF, Kim MS, Vakifahmetoglu-Norberg H, Yuan J. Deubiquitination of NLRP3 by BRCC3 critically regulates inflammasome activity. *Mol Cell.* 2013; 49:331–38.
<https://doi.org/10.1016/j.molcel.2012.11.009>
PMID:23246432
27. Duong BH, Onizawa M, Osés-Prieto JA, Advincula R, Burlingame A, Malynn BA, Ma A. A20 restricts ubiquitination of pro-interleukin-1 β protein complexes and suppresses NLRP3 inflammasome activity. *Immunity.* 2015; 42:55–67.
<https://doi.org/10.1016/j.immuni.2014.12.031>
PMID:25607459
28. Ohlsson BG, Englund MC, Karlsson AL, Knutsen E, Erixon C, Skribeck H, Liu Y, Bondjers G, Wiklund O. Oxidized low density lipoprotein inhibits lipopolysaccharide-induced binding of nuclear factor-kappaB to DNA and the subsequent expression of tumor necrosis factor-alpha and interleukin-1beta in macrophages. *J Clin Invest.* 1996; 98:78–89.

- <https://doi.org/10.1172/JCI118780> PMID:[8690807](https://pubmed.ncbi.nlm.nih.gov/27931771/)
29. Miller YI, Shyy JY. Context-Dependent Role of Oxidized Lipids and Lipoproteins in Inflammation. *Trends Endocrinol Metab.* 2017; 28:143–52.
<https://doi.org/10.1016/j.tem.2016.11.002>
PMID:[27931771](https://pubmed.ncbi.nlm.nih.gov/27931771/)
30. Cavey JR, Ralston SH, Hocking LJ, Sheppard PW, Ciani B, Searle MS, Layfield R. Loss of ubiquitin-binding associated with Paget’s disease of bone p62 (SQSTM1) mutations. *J Bone Miner Res.* 2005; 20:619–24.
<https://doi.org/10.1359/JBMR.041205>
PMID:[15765181](https://pubmed.ncbi.nlm.nih.gov/15765181/)
31. Sergin I, Evans TD, Zhang X, Bhattacharya S, Stokes CJ, Song E, Ali S, Dehestani B, Holloway KB, Micevych PS, Javaheri A, Crowley JR, Ballabio A, et al. Exploiting macrophage autophagy-lysosomal biogenesis as a therapy for atherosclerosis. *Nat Commun.* 2017; 8:15750.
<https://doi.org/10.1038/ncomms15750>
PMID:[28589926](https://pubmed.ncbi.nlm.nih.gov/28589926/)
32. Zaffagnini G, Savova A, Danieli A, Romanov J, Tremel S, Ebner M, Peterbauer T, Sztacho M, Trapannone R, Tarafder AK, Sachse C, Martens S. p62 filaments capture and present ubiquitinated cargos for autophagy. *EMBO J.* 2018; 37:37.
<https://doi.org/10.15252/emboj.201798308>
PMID:[29343546](https://pubmed.ncbi.nlm.nih.gov/29343546/)
33. Sun D, Wu R, Zheng J, Li P, Yu L. Polyubiquitin chain-induced p62 phase separation drives autophagic cargo segregation. *Cell Res.* 2018; 28:405–15.
<https://doi.org/10.1038/s41422-018-0017-7>
PMID:[29507397](https://pubmed.ncbi.nlm.nih.gov/29507397/)
34. Song H, Liu B, Huai W, Yu Z, Wang W, Zhao J, Han L, Jiang G, Zhang L, Gao C, Zhao W. The E3 ubiquitin ligase TRIM31 attenuates NLRP3 inflammasome activation by promoting proteasomal degradation of NLRP3. *Nat Commun.* 2016; 7:13727.
<https://doi.org/10.1038/ncomms13727>
PMID:[27929086](https://pubmed.ncbi.nlm.nih.gov/27929086/)